Probabilistic Fracture Simulation

A SEMINAR REPORT

Submitted in the partial fulfillment of the award of the degree of

MASTER OF TECHNOLOGY

in

STRUCTURAL ENGINEERING

By

ABHINANDAN SHARMA

Under the Guidance of

PROF. RAJIB CHOWDHURY

STRUCTURAL ENGINEERING GROUP

DEPARTMENT OF CIVIL ENGINEERING

INDIAN INSTITUTE OF TECHNOLOGY ROORKEE

ROORKEE- 247667, UTTARAKHAND, INDIA.

MAY 2021

INDIAN INSTITUTE OF TECHNOLOGY ROORKEE
ROORKEE - 247667

CANDIDATE'S DECLARATION

I hereby declare that work being presented in this report, entitled **"Probabilistic Fracture Simulation"** towards partial fulfillment of the requirements for the award of the degree of **"Master of Technology in Structural Engineering"** submitted to the Department of Civil Engineering, Indian Institute of Technology, Roorkee, is an authentic record of my own work carried out under the guidance of **Dr. Rajib Chowdhury**, Associate Professor, Department of Civil Engineering, IIT Roorkee.

The matter presented in this thesis has not been submitted by me for the award of any other degree of this or any other Institute.

Date: **(ABHINANDAN SHARMA)**
Place:

COUNTERSIGNED

This is to certify that the above statement made by the candidate is correct to the best of my knowledge.

Date:
Place:

Dr. Rajib Chowdhury
Associate Professor,
Department of Civil Engineering,
Indian Institute of Technology,
Roorkee
Roorkee – 247667 (INDIA)

INDIAN INSTITUTE OF TECHNOLOGY ROORKEE
ROORKEE - 247667

ACKNOWLEDGEMENT

I would like to thank and express my deepest sense of gratitude and indebtedness to my M.Tech. supervisor **Dr. Rajib Chowdhury**, Associate Professor, Department of Civil Engineering, IIT Roorkee, for his valuable guidance, encouragement and generous assistance throughout in putting together this seminar report. This work is simply the reflection of his thoughts, ideas, concepts and all his efforts. I am highly indebted to him for his kind and valuable suggestions and of course his valuable time during the period of the work.

I would acknowledge my gratefulness to my seniors and friends who provided valuable suggestions and encouragement whenever I needed. I am also extremely grateful to my family members for their support, love, patience and for being a constant source of inspiration.

Date: **ABHINANDAN SHARMA**

Contents

List of Figures

Abstract

This seminar topic focuses on the Fundamentals of the fracture mechanics based on the crack tip stress and strain fields and the non-linear fracture mechanics have been developed. Their applications to the studies of fracture initiation and stable crack growth may differ because of the difference in the basic postulates of various fracture theories. the impact of computational methodology on furthering the understanding of fundamental fracture phenomena. The current numerical approaches to the solution of fracture mechanics problems. the methodology for probabilistic fracture mechanics analysis (PFM) of structural components with crack-like imperfections. Details are given for the development and application of both a simple nomographic method and a basic numerical tool for PFM applications.

1 Fundamental Basis Of Fracture Mechanics

Inglis made the stress analysis of an elliptical hole in a uniformly stressed elastic plate. A crack can be represented by an infinitesimally narrow ellipse. Based on Inglis elastic stress solution to a cracked solid. Griffith formulated his well known energy criterion for brittle fractures. At the fracture initiation of a cracked brittle solid in the condition of fixed grip, the release rate of the stored strain energy equals or exceeds the dissipative surface energy rate. $\partial U_\epsilon/\partial a \geq \partial U_s/\partial a = 2\gamma$, where U_ϵ and U_S are strain energy and surface energy; γ, the surface energy per unit area; and a, crack length.γ is constant for a given material. Assuming a constant dissipative rate of plastic energy Γ , Irwin and Orowan extended the energy criterion to metallic solids, where plastic deformation takes place at crack tips.

The crack tip elastic stresses, strains and displacements are characterized by the stress intensity factor, K. Incase of small scale yielding, SSY, K characterizes crack tip stresses, strains, and displacements even within a crack tip plastic zone in a metallic specimen. K characterizes cracktip stresses, strains and displacements forms the fundamental basis of the linear elastic fracture mechanics rather than the global energy balance. More recently, Hutchinson, and Rice and Rosengren derived the crack tip stress, strain and displacement fields in power law strain hardening materials. The crack tip stress, strain and displacement fields can be characterized by J, which is a contour independent integral. J is also the rate of potential energy change during the cracking process in a non-linear elastic solid. J has been widely used to study non-linear fracture mechanics.

1.1 Defining Fracture

Figure shows a cracked sample and its load P vs load point displacement, δ. The “crack” suddenly starts to propagate internally at A. The increased crack length increases the compliance of the specimen and causes the sudden load drop from A to A’. As the load increases, the crack continues its internal growth. At B, the crack front at the specimen surface starts to move forward, and the crack continues to grow in a “stable” manner to the maximum load C. D is the point of final separation, fracture mechanics studies the fracture initiation at A and the stable crack growth from A’ to B and onwards. Often the point of fracture initiation is not so clearly defined as shown in the figure. In this case, certain degree of arbitrariness has to be introduced in order to define fracture initiation. Fracture can be defined in terms of the above described macro-features or in terms of the micro-structural features such as fracture of brittle inclusions,etc.

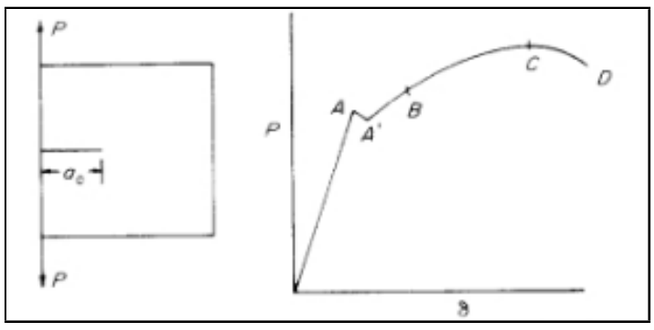

load-elongation curve for fracture initiation and stable crack growth

1.2 Elastic Stress Field

Linear elastic fracture mechanics (LEFM) is based on the elastic solution of the crack tip stress field. Williams has shown that in a cracked plate σ_{ij}, ϵ_{ij} and u_i can be expressed in terms of:

$$\sigma_{ij}(r,\theta) = \frac{k_1}{\sqrt{2\pi r}}\bar{\sigma}_{ij(1)}(\theta) + k_2\bar{\sigma}_{ij(2)}(\theta) + k_3\sqrt{(2\pi r)}\bar{\sigma}_{ij(3)}(\theta) + ...$$
$$\epsilon_{ij}(r,\theta) = \frac{k_1}{\sqrt{2\pi r}}\bar{\epsilon}_{ij(1)}(\theta) + ... \quad (1)$$
$$u_{ij}(r,\theta) = \frac{k_1\sqrt{(2r)}}{\pi}\bar{u}_{i(1)}(\theta) + ...$$

where r and θ are polar coordinates, the crack tip is located at the origin of the reference system, and the crack line coincides with the line $\theta = \pi, \bar{\sigma}_{ij}, \bar{\epsilon}_{ij}$ and $, \bar{u}_i$ give the distributions of their corresponding stress, strain, and displacement components. $k_1, k_2, k_3...$ are prescribed by specimen geometry and boundary conditions. Fracture takes place at the crack tie: therefore, we have to consider only the stresses and strains in the immediate vicinity of a crack tip. In this region, the first singular terms of these series dominate the stress and strain fields. Irwin writes these singular terms for mode I tensile cracks in the following form:

$$\sigma_{ij}(r,\theta) = \frac{K_I}{\sqrt{2\pi r}}\bar{\sigma}_{ij}(\theta)$$
$$\epsilon_{ij}(r,\theta) = \frac{K_I}{\sqrt{2\pi r}}\bar{\epsilon}_{ij}(\theta) \quad (2)$$
$$u_{ij}(r,\theta) = \frac{K_I\sqrt{(2r)}}{\pi}\bar{u}_i(\theta)$$

The elastic stress or strain field can be separated into two parts dealing with stress distribution and is a function of the coordinates alone. In cracked solids this is $\bar{\sigma}_{ij}(\theta)/\sqrt{(2\pi r)}$ and the other part is K, or the "stress intensity factor". If K_I is known, all $\bar{\sigma}_{ij}, \bar{\epsilon}_{ij}$ and $, \bar{u}_i$ are known. Therefore, K_I characterizes crack tip stresses, strains, and displacements. Equatione (2) approximates characteristic creack tip elastic field zone, r_e

As a crack propagates, the stored strain energy in the plate changes. The strain energy change can be calculated. Figure shows the contour of a crack tip under stress. Apply stress σ_{yy} in the crack increment Δa. As σ_{yy} increases, the two mating crack surfaces close. The necessary work done to close the crack within Δa is:

$$\Delta W = \int_0^{\Delta a} \sigma_{yy}(r',0)u_y(r,\pi)dr = \frac{(1-\nu^2)}{E}K_I^2\Delta a \quad (3)$$

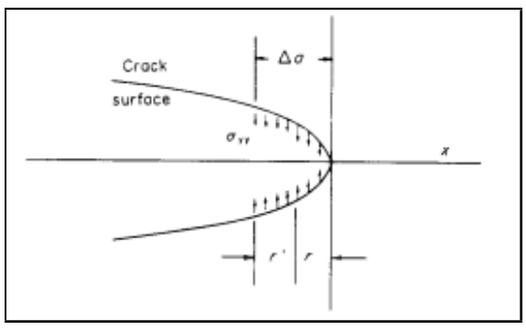

word done to close the crack increment Δa

for the plane strain case. This is also the amount of strain energy released as the crack moves forward under the fixed grip condition. It can be considered as the strain energy flux which flows toward the crack tip during fracturing.

The rate of the strain energy flux is denoted by G and is also known as crack extension force.

$$G_I = K_I^2/\bar{E} \quad (4)$$

where $\bar{E} = E/(1-\nu^2)$ for plain strain case and $\bar{E} = E$ for plane stress.

1.3 Griffith Criterion

Griffith proposed the criterion of brittle fracture based on the principle of global energy balance.

$$\frac{\partial}{\partial a}(U_\epsilon + U_\gamma) = 0 \quad (5)$$

where U_ϵ is the strain energy and U_γ is the surface energy.

$$G = -\frac{\partial U_\epsilon}{\partial a}$$
$$and$$
$$\frac{\partial U_\gamma}{\partial a} = 2\gamma$$

which is constant. For a small crack in a large plate, we habbve, at fracture.

$$G_c = (1-\nu^2)\frac{\sigma_c^2 \pi a}{E} = 2\gamma$$
$$and$$
$$\sigma_c = \sqrt{\frac{2\gamma E}{(1-\nu^2)\pi a}}$$

Hence, $\sigma_c\sqrt{(\pi a)} =$ material constant

Hence, for perfectly brittle solid k characterizes σ_{ij} and ϵ_{ij}. For same material and same crack tip elastic stresses and strains, the K_c(critical value) must be constant.

$$K_c = \sigma_c\sqrt{(\pi a)} = \text{constant}$$

1.4 The Extension Of The Griffith Criterion

A correct fracture theory should agree with know fracture phenomena. If not, the analysis must be wrong. The fracture stress, σ_c, of a large specimen with a long crack is lower than the fracture stress of a small specimen with a short crack as shown schematically in figure below.

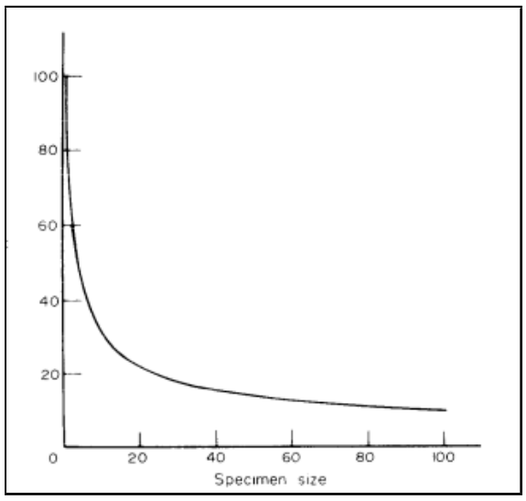

Fracture stress of geometrically similar specimens, same thcikness, same material

1.4.1 Global Energy Balance Theory

At fracture we have:

$$\frac{\partial}{\partial a}(U_\gamma + U_\epsilon + U_p) = 0 \tag{6}$$

U_γ is surface energy; U_ϵ is strain energy; and U_p is plastic work. It is known that $U_\gamma \ll U_p$. Neglect U_γ, we get:

$$\frac{\partial}{\partial a}(U_\epsilon + U_p) = 0 \tag{7}$$

This leads to $G_c = (\partial U_p/\partial a)$. In infinite metallic plate in the condition that strain prevails due to enough thickness. As cracks extend under σ_∞, the relation between work dissipation U_p and crack lengh "$2a$" can be found. The classic plasticity theory shows, $r_p \propto a$, and $U_p \propto r_p^2$ which gives

$$\frac{\partial U_p}{\partial a} = Ca$$

C is proportionality constant, which gives:

$$\frac{\sigma_c^2 \pi a(1-\nu^2)}{E} = Ca \qquad \Rightarrow \qquad \sigma_c = \sqrt{\frac{CE}{\pi(1-\nu^2)}} = \text{constant}$$

The experimental evidences that demonstrate the failure of the global energy balance are well known. But they have not been recognized as such. Figure shows the thickness effects on fracture toughness. The fracture toughness varies from 40 MPa$\sqrt{\text{m}}$ for K_{Ic}, to the maximum value of 107 MPa$\sqrt{\text{m}}$. The strain energy release rates of the two limiting cases of plane strain and plane stress states differ by a factor of $(1-\nu^2)$. v is Poisson's ratio. The difference is approximately 10%. If the plastic energy dissipation rate is constant, the difference in fracture toughnesses should not be more than 10%. The large difference in the observed fracture toughnesses in Figure, from the point of view of energy balance, must arise from the difference in plastic energy dissipation rates.

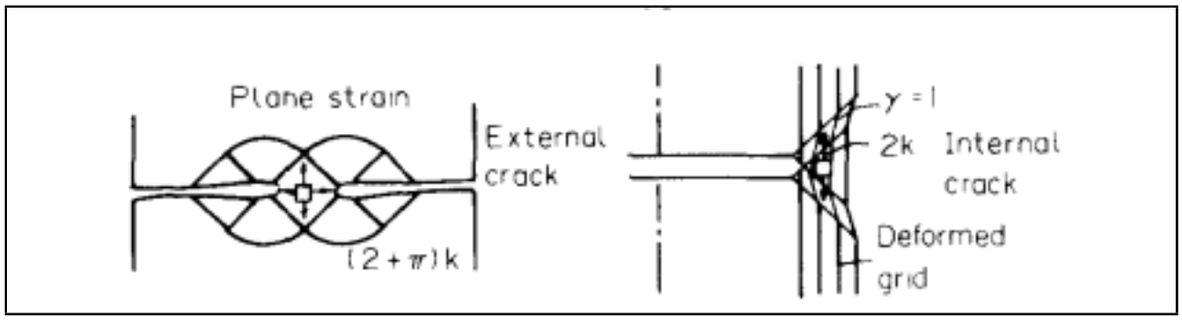

Thickness effect on fracture toughness

In order to explain the observed experimental phenomena, it is necessary to resort to the difference in the state of crack tip stress field. The lower plastic energy dissipation rate in the state of plane strain is caused by the triaxial state of tensile stress, which causes reductions in effective stress, plastic deformation, and plastic energy dissipation; and it causes an increase in maximum tensile stress and an earlier fracture initiation. The data clearly indicate that when the crack tip fields of the effective stress and the maximum tensile stress change, the fracture toughness will vary.

Additional evidences of the failure of global energy balance theory are shown by the results of fracture under combined load. If plastic energy dissipation rate is constant, at the point of fracture initiation, $(\text{G}_I + \text{G}_{II} + \text{G}_{III})$ must be a constant. Experimental evidences have shown that this is far from universally true [12]. It is evident that if K fails to characterize the same crack tip field, the global energy balance theory fails to work. Therefore the criterion of global energy balance for fracture initiation without the consideration of the state of crack tip stresses and the detailed fracture processes, must be fortuitous. The global energy balance theory is more suitable to the analysis of the final fracture when the three dimensional effects of crack tip stresses and strains and the associated material responses are taken into consideration.

1.4.2 Sharp Notch Analysis

All crack tips are "blunted," so sharp notches and cracks can be considered as equivalents. We will consider sharp elleptical notches in large plates under tensile loading in a direction perpendicular to the major axis.

The fracture stress of a notched specimen depends on notch root radius, R, as shown schematically in Figure. σ_c decreases with R. However, if the notch root radius is less than a certain value R_c,$\sigma_c$is no longer R dependent. When a solid contains a sharp notch of initial root radius R_i, the radius increases with the applied load. If the root radius increment, ΔR is much larger than R_i, the fracture stress σ_c is independent of R_i. If the size of the fracture process zone, ρ_F is much larger than R_i, σ_c will also be independent of R_i. In our analysis, we assume R is always less than R_c.

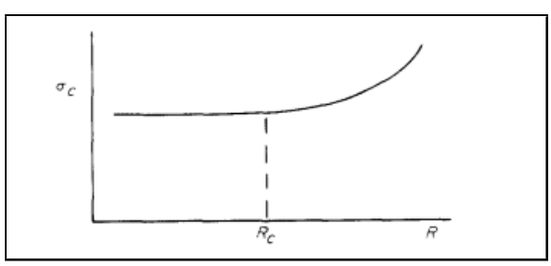

Fracture stress as a function of crack tip radius

Let us consider geometrically similar elliptical notches in geometrically similar specimens. The major axis of the ellipse is $2a$. All the specimens are stressed to the same value of σ_c. In this case, each component of

σ_{ij} or ϵ_{ij} in all of these specimens has the same value at the geometrically similar points, $P((r/a), \theta)$. If σ_{ij} or ϵ_{ij}control the fracture process and if one specimen fails at a given σ_∞ all the specimens should fail at the same applied stress σ_∞, which again contradicts the experimental observations.

1.4.3 The Theory Of K-characterization

Under the condition of small scale yielding, SSY, K characterizes the crack tip stresses and strains even within r_p. Let us illustrate this with two samples of different geometry but they are loaded to the same K-value. These samples are made of the same material and have the same thickness

Within the region of $r_c(\theta)$ near the cack tip, the singular terms, $\sigma_{ij} = (K/\sqrt{(2\pi r)}\bar{\sigma}_{ij}(\theta))$ dominate the stress field. r_e is the characteristic elastic crack field zone. For elastic solids, if $r_{e1} = r_{e2}$ the boundary stresses on r_{e1} and r_{e2} must be equal to each other, since $K_1 = K_2$.

In metallic specimens, closer to the crack tip, plastic deformation takes place within $r_p(\theta)$. Let us examine the regions within r_{e1} and r_{e2} as free bodies given below:

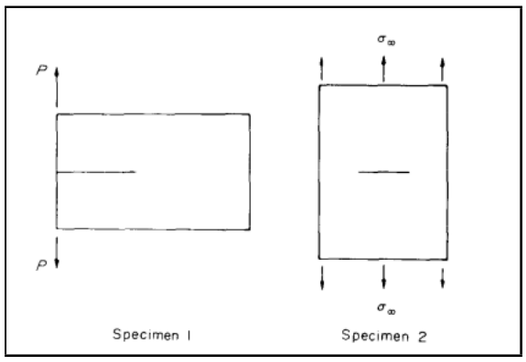

Two different fracture toughness specimens, $K_1 = K_2$

In our case, $r_{e1}(\theta) = r_{e2}(\theta)$. If $r_p \ll r_e$ the stress relaxation within r_p does not disturb much the boundary stresses on r_e, therefore, the boundary stresses on r_e are essentially those given by the singular terms of the linear elastic solution. Since $K_1 = K_2$, the boundary stresses on these two free bodies must be the same. With the same geometric shape and size and the same boundary stresses, we must have:

$$\begin{aligned} \sigma_{ij}(r,\theta)_1 &= \sigma_{ij}(r,\theta)_2 \\ \epsilon_{ij}(r,\theta)_1 &= \epsilon_{ij}(r,\theta)_2 \end{aligned} \tag{8}$$

K_c is invariant to planar geometric variation.

$$\begin{matrix} a \\ L \end{matrix} \geq 2.5 \left(\frac{K_c}{\sigma_c}\right)^2 \tag{9}$$

The crack tip σ_{ij} and ϵ_{ij} are not only affected by the planar dimensions of "a" and "L". They are also strongly affected by the specimen thickness, t.The size requirements needed to satisfy the condition of SSY and that of plane strain are

$$\begin{matrix} t \\ a \\ L \end{matrix} \geq 2.5 \left(\frac{K_c}{\sigma_c}\right)^2 \tag{10}$$

The condition of $r_e \gg r_p$ is known as the condition of small scale yielding. Wilson has found that the size of r_e is quite small when compared with other specimen dimensions, only a few per cent of other planar dimensions of a sample. However, $r_e \propto specimen\ size$; so, in principle, the condition of SSY can always be satisfied by using a large enough sample. The condition of r_e is a sufficient but not necessary condition for the validity of the LEFM. The condition could be unduly restrictive in terms of specimen size requirements. The necessary condition for the validity of the linear elastic fracture mechanics is that K would be able to characterize the crack tip stress or strain component at the location of the defined fracture process.

1.5 Fracture Process Zone

Materials are inhomogeneous. They contain brittle and ductile phases, inclusion particles, grain boundaries, etc. Fracture initiation in a cracked solid is often in the interior of a specimen, where the high tensile stress

exists at the locations of brittle and weak materials. Once a local fracture is initiated, it spreads out. For example, local fracture may start at inclusion 1 (Figure below). The fracture at inclusion I increases the stress at inclusion 2, and the increased stress causes the fracture of inclusion 2. Ductile fracture takes place between the brittle particles. If the brittle inclusions are large and closely spaced, it may cause an avalanche effect, one particle fracturing rapidly after the other. The fracturing process stops when the crack is out of the zone of the high tensile stress in the plane strain triaxial state of tension. The crack extension could be sizable and could cause noticeable load drop. This is the well known phenomenon of pop-in and is a $local\ instability$. Hence, K_{Ic} is the result of a local instability phenomenon, not a global instability.

Local fractures may also occur through interface separation between particles and matrix; it may occur at the embrittled grain boundary, where a high enough tensile stress exists in the plane of the embrittled grain boundary. The weakened grain boundary may be caused by temper embrittlement, hydrogen embrittlement, and embrittlement by O_2, Cl_2 or other chemicals.

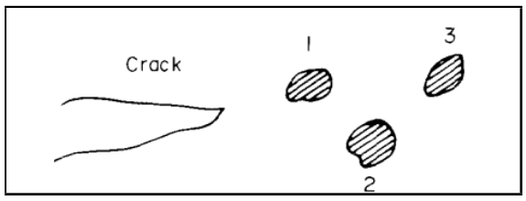

Brittle inclusions ahead of a crack tip.

Both fracture initiation and stable crack growth are phenomena of local instability. Therefore, the local energy balance rather than the global energy balance should be used. In order to do so, we need to treat materials as inhomogeneous substances.

The condition of small scale yielding, that enables K to characterize crack tip stresses and strains responsible for the fracture process, gives the size requirements for the linear elastic fracture mechanics eqns (9) and (10). In addition, we should impose the condition

$$\rho_F < r_e \tag{11}$$

for composite materials. The J-integral removes the requirements for a and L. But an additional size requirement

$$\rho_F < r_{cp} \tag{12}$$

needs to be imposed for metallic fractures. A thickness requirement is also needed for plane strain case.

1.6 Fracture Toughness And Fracure Ductility

The initiated local fracture will continue to propagate. The extent of fracture propagation varies according to the "brittleness" of the material. The fracturing processes can be classified in three categories.

(1) Once initiated, the localized fracture will continue to grow rapidly across the specimen without further increase in σ_∞ or K. It is very brittle.

(2) Once initiated, the localized fracture will continue to grow to a sizable extent in a rapid manner while (σ_∞ and K drop. After the initial fracture, it needs to increase K in order to continue to grow further. Fracture is initiated in the interior in the plane strain region, and the initial fracturing process will stop when the crack is out of the zone of triaxial state of tension.

(3) If fracture initiation is caused by brittle particles and if the brittle particles are small and far apart, once the local fracture is initiated, it needs a considerable amount of plastic deformation to grow across the regions between particles. A crack grows primarily by the process of plastic deformation. This material is ductile and tough.

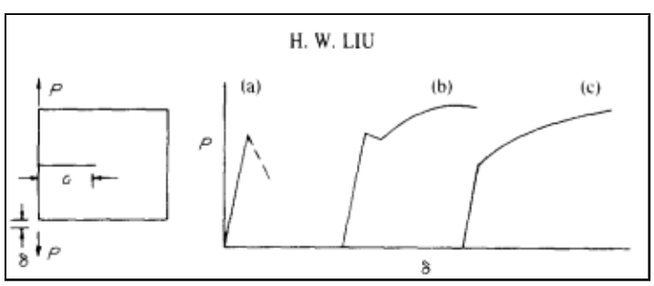

Schematic diagrams of load vs load point displacement showing difference in fracture ductility

K and J characterize σ_{ij} and ϵ_{ij} within the fracture process zone. The maximum tensile stress, $\sigma_{\max}$, could be the parameter that controls fracture initiation in the case of brittle particles, The nucleated crack may then propagate rapidly for a clear definition of K_{lc}. as shown in Fig. (a) and (b). In this case, K_{lc} might be correlated with $\sigma_{\max}$. On the other hand, if the particles are small and far apart, the nucleated minute local fractures will grow by a mechanism which needs a great deal of plastic deformation. If K_{lc} is defined by a specific amount of crack growth, primarily by a mechanism of plastic deformation, K_{lc} will be correlated better with the effective plastic strain, $\bar{\epsilon}^p$. If a crack propagates by the shear-off process between the ductile matrix and hard second phase, then the maximum shear strain should be used. The beauty of both of the linear and non-linear fracture mechanics, is that both the K and J can be used in all of the illustrated cases, because K and J characterize all the stress and strain components, as well as their combinations such as $\bar{\sigma}$, $\sigma_{\max}$, $\bar{\epsilon}^p$, $\gamma_{\max}$, and strain energy density if the condition of $\rho_F < r_{cp}$is satisfied.

K and J are macro-parameters. As long as they can characterize the stresses and strains at the location of fracture initiation and fracture propagation, they can be used to measure fracture toughness regardless of the details of the initiation and propagation processes. Clearly, we use K and J as indirect parameters which do not infer any specific fracture process.

---

2 Computational Fracture Mechanics

This topic focuses on the impact of computational methodology on furthering the understanding of fundamental fracture phenomena. The current numerical approaches to the solution of fracture mechanics problems, e.g. finite element (FE) methods, finite difference methods and boundary element methods, are reviewed. The application of FE methods to the problems of linear elastic fracture problems is discussed. A special focus is placed on stable crack growth problems. The need for further research in this area is emphasized. The importance of large strain phenomena and accurate modelling of non-linearities is highlighted. An expanded version of fracture mechanics methodology is given by Liebowitz *[Advances in Fracture Research 3. Pergamon Press, Oxford (1989)]*; additional treatment is given in this paper to numerical results incorporating error estimates and algorithms for mesh design into the FE code. The adaptive method involves various stages which includes FE analysis, error estimation/indication, mesh refinement and fracture/failure analysis iteratively.

2.1 Numerical Methods For Solution Of Fracture Problems

The problems of fracture mechanics reduce to the solution of boundary value problems (which may be static or dynamic) which have mixed boundary conditions. The shape and the mixed boundary conditions can give rise to singularities in the stress and strain fields. The problems may involve both material and geometric non-linearities, which complicate the formulation and render prediction of convergence extremely difficult. Because little can be done with these problems analytically, numerical methodologies are required.

The *finite difference* method is the oldest technique for the solution of boundary value problems. The method directly involves the solution of the governing differential system in an approximate manner by subdividing the domain of interest into a connected series of discrete points called nodes. These nodes are the sampling points for the solution and are linked using the finite difference operators to the governing equations. Employment of the finite difference operators results in a system of algebraic equations for the discrete nodal values of the field variable. The finite difference method can be used to discretize both space and time. The finite difference method is difficult to use for irregularly shaped domains or for problems involving singularities, because the fine meshing required near a singularity cannot easily be reduced for the rest of the domain.

Integral equation methods basic approach employed involves an analytic formulation of the elasticity problem to the point of a singular integral equation. The singularity is then extracted and the result is a non-singular integral equation which can be solved quite accurately with any number of techniques. This approach yields excellent solutions; however, it requires an extensive analytic formulation which is different for each new problem. The method is quite useful, nonetheless, for establishing benchmark solutions to compare with other methods as the degree of accuracy can be guaranteed. The method is only applicable to elasticity problems (without non-linearities). For three-dimensional problems, the derivation of the integral equations becomes quite laborious.

The *Boundary Integral Equation Method* (BIEM) is a numerical approach to the solution of linear boundary value problems with known Green's function solutions. The boundary of the domain of interest is discretized using "elements" which are interconnected at discrete points called nodes. For a three-dimensional problem, the mesh is two-dimensional; for two-dimensional problems, the mesh is one-dimensional. The boundary

value problem is formulated as an equivalent surface or line integral using the Green's function solution and the governing differential system. For linear elasticity in two dimensions, the formulation is based on Betti's theorem and the resulting system of equations is given by

$$C_{ij}u_j + \int_\Gamma T_{ij}u_j \, d\Gamma + \int_\Gamma U_{ij}t_j \, d\Gamma \tag{13}$$

where U_i and t_i are the surface displacement and traction vectors on the domain boundary, and U_{ij} and T_{ij} are related to the Green's function solutions for displacements and tractions, respectively. At each boundary point, either u_j is specified (on Γ_u) or t_j is specified on (Γ_t), while the variable is unknown. For static problems, the BIEM reduces to the solution of a system of dense linear equations which may be non-symmetric. If surface data are the only quantities required,the BIEM is often computationally superior to the FEM for two-dimensional problems. If interior data are required, the method is computationally costly. For three-dimensional problems, BIEM solutions are often very expensive as the resulting linear system is dense, unbanded and often non-symmetric, and often do not produce good solutions.

The *Finite Element Method* is the most widely employed numerical method for fracture mechanics problems. The formulation of the FEM is based on a variational statement of the governing physics. For the problems of linear elasticity, the Principle of Virtual Work, given by

$$\int_v \sigma_{ij}\delta\epsilon_{ij}\mathrm{d}V = \int_S \sigma_{ij}n_j\delta u_i\mathrm{d}S \tag{14}$$

which is employed, where σ_{ij} is the stress tensor, $\delta\epsilon_{ij}$ is the virtual strain tensor due to virtual displacements δu_i and n_j is the normal vector to the surface of applied tractions. The domain is discretized into subdomains (elements) which are interconnected through common discrete points (nodes). The primary unknown field variables are nodal values. The formulation reduces the problem to the solution of a system of algebraic equations in terms of the nodal variables (for dynamic problems, the result is a system of ordinary differential equations). Finite element systems tend to be relatively banded and symmetric for most problems.For fracture mechanics problems, the FEM can be employed in the standard manner or modified to account for the singular nature of the near crack fields.

Method	Strengths	weaknesses
Finite difference	Easy to employ Error estimates available	Slow convergence Uniform mesh requirement Cannot model singularities
Finite elements	Good convergence Singularities can be modeled	Modeling is difficult Few existing error estimators
Boundary element	Modeling is easier Error estimation is easy	computationally more expensive Converges slowly for singular problems
Hybrid approaches	Good for specific problems Generally very accurate	Usually developed for restricted problem class difficult to implement

2.2 Impact Of FEM On LEFM

2.2.1 Stress Intensity Factors

The ability to predict accurately the stress intensity factors for cracked elastostatic bodies using standard numerical techniques has greatly advanced the use of LEFM concepts in application. Most commercial FEM and BIEM codes have two-dimensional elastostatic fracture capabilities built-in and automated.

The prediction of three-dimensional stress intensity factor distributions is not a straightfor- ward process. Research in this area has been ongoing for more than 10 years. Special singular elements have been proposed by Tracey , Blackburn and Hellen, Hilton and others. These singular elements are based on employment of the asymptotic displacement field in the finite element formulation directly. The element geometry is the same as the corresponding standard elements. As analyzed elsewhere, these approaches require the assumption

of a local state of plane strain near the crack front which has not been established analytically. They must be utilized, therefore, with discretion.

Once the FE field solutions are obtained, there are essentially two approaches to calculate the stress intensity factors: the multi-term displacement field approach and the nodal force approach. These approaches are based on the asymptotic displacement field and stress field near the crack front, given as

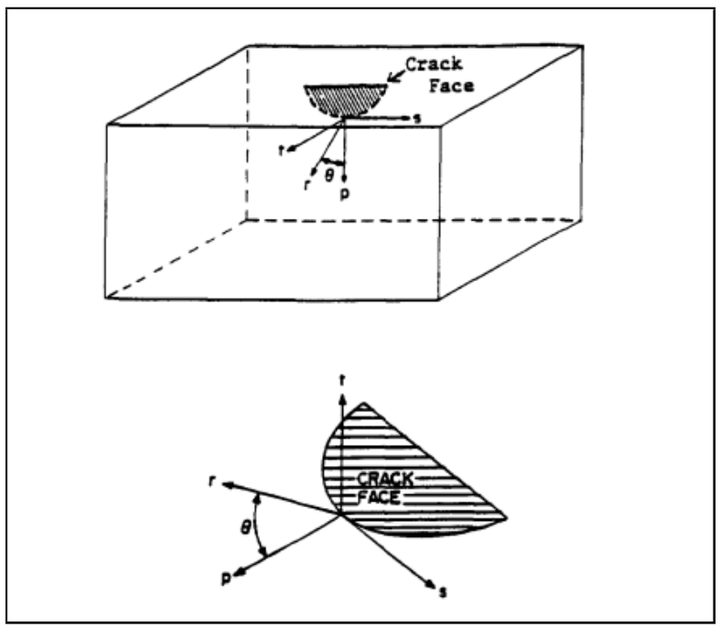

Three-dimensional crack geometry.

$$u_1^1 = \left(\frac{1+\nu}{E}\right)\left(\frac{2r}{\pi}\right)^{1/2}\left\{K_I \cos\frac{\theta}{2}\left[(1-2\nu)+\sin^2\frac{\theta}{2}\right] + K_{II}\sin\frac{\theta}{2}\left[2(1-\nu)+\cos^2\frac{\theta}{2}\right]\right\}$$

$$u_2^1 = \left(\frac{1+\nu}{E}\right)\left(\frac{2r}{\pi}\right)^{1/2}\left\{K_I \sin\frac{\theta}{2}\left[2(1-\nu)+\cos^2\frac{\theta}{2}\right] - K_{II}\cos\frac{\theta}{2}\left[2(1-\nu)+\sin^2\frac{\theta}{2}\right]\right\}$$

$$u_2^1 = 2\left(\frac{1+\nu}{E}\right)\left(\frac{2r}{\pi}\right)^{1/2} K_{III}\sin\frac{\theta}{2} \tag{15}$$

$$\sigma_{ij} = \frac{K_I}{\sqrt{r}}f_{ij}(\theta) + \frac{K_{II}}{\sqrt{r}}g_{ij}(\theta) + \frac{K_I}{\sqrt{r}}f_{ij}(\theta) + \frac{K_{III}}{\sqrt{r}}h_{ij}(\theta) \tag{16}$$

where f_{ij}, g_{ij} and h_{ij} are known functions of θ; the local coordinate system is defined. It should bementioned that, due to the assumption of local plane strain in the neighborhood of the crack front, the multi-term displacement method can yield erroneous results where crack front curvatures are large or as the crack front approaches a free surface.

2.2.2 Energy Release And J-integral

The Griffith energy release theory of LEFM is widely accepted as a criterion for fracture proof design. This theory involves the calculation of the amount of energy released with a virtual extension of the crack. The criterion originally proposed by Griffith requires that the crack can be idealized as a line of discontinuity and that the remote loading is tensile and normal to the crack. In other words, it is restricted to a two-dimensional linear, elastic mode I fracture problem. In such a case, it is well known that the energy release rate can be related to the stress intensity factor K_1 and the path independent J-integral as follows:

$$G = J = \pi(\kappa+1)K_I^2/8\mu \tag{17}$$

where $\kappa = 3-4\nu$ for plane strain and $\kappa = (3-\nu)/(1+\nu)$ for generalized plane stress; the J-integral is defined as

$$J = \int_\Gamma (U(d)y - \sigma_{ij}n_j u_{i,x}\mathrm{d}s) \tag{18}$$

For two-dimensional mixed mode fracture problems, if the crack is to extend along the line of the crack, i.e. self-similar crack extension, then the $G-J-K$ relation is given as

$$G = J = \pi(\kappa+1)(K_I^2+K_{II}^2)/8\mu \tag{19}$$

If the line of crack extension deviates from the crack line by an angle θ, then the energy release rate is obtained as

$$G(\theta) = \pi(\kappa + 1)(1 + c)[K_1^2(1 + c) + K_{11}^2(5 - 3c) - 4K_1K_{11}s]/32\mu \tag{20}$$

It is emphasized that the energy release rate theory originally proposed by Griffith is now generalized; eq. (20) is the general $G - K$ relation; the value of G_{max} is greater than that of G obtained from eq. (19) for self-similar crack extension; and G_{max} is greater than the value of the J-integral and hence it is fair to say that the J-integral is only applicable to self-similar crack extension problems.

2.2.3 Dynamic Crack Propogation

In addition to the study of static LEFM problems, much work has been performed for dynamic LEFM problems. In the dynamic case, two problems are important: that of a running crack and that of a static crack with elastic waves impinging. The problem of stress intensity factor calculation for static cracks in elastic materials subjected to time-dependent loading is no more difficult than the corresponding static problem. The same solution methodologies are employed and the results can be calculated to the same accuracy. Computational requirements are greater; however, no new problems arise numerically. The problem of a running crack in an elastic material is much different from the problem of a static crack. FEM solutions have had a major impact on this area. Few analytic solutions to realistic problems are available (even in two dimensions); therefore, robust numerical approaches are essential. The first realistic solution to the problem of a running crack was presented by Anderson. They introduced a nodal release algorithm which models the changing boundary conditions of a growing crack. The method has proved to be very robust and easy to implement, even in commercial finite element codes, and is widely employed. This algorithm has allowed many researchers to study running crack problems for a wide variety of geometries and loadings. An interesting example of dynamic crack propagation simulation involves the problems of interacting cracks. Consider the problem of two cracks in a sheet which are opened by wedge loads. The cracks at two sides of the sheet are slightly misaligned to provide initial asymmetry. Figure shows the cracks at three stages of the analysis. Initially, the cracks repel each other and, as propagation continues, they attract. At the final stage, the two cracks intersect. Figure shows the stress intensity factor histories as a function of crack length. The positive mode II component is evident during the avoidance stage and negative mode II is evident during attraction.

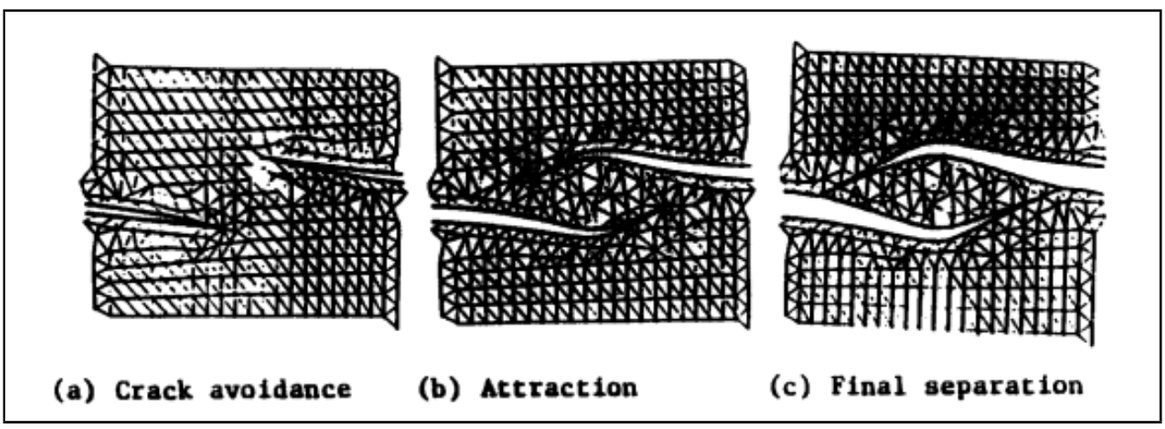

Displacement plots during crack propagation

2.3 Adaptive Finite Element Analysis

One of the biggest problems with finite element analysis (FEA) lies in the fact that an assessment of the reliability of the FE solution is difficult to obtain. The FE analyst is usually guided by experience in designing and assessing the quality of the mesh. After solution, simple checks, such as examining the stress discontinuities between elements, can be made to assess the quality of the solution. Based on the analyst's experience the solution is accepted or rejected. If this approach can be automated, not only would the solution be improved but a large saving in man-hours would be made.

The projection or stress smoothing type error estimators are a global measure of the discretization error contained in any given FEA. For adaptive schemes the local error does tend to approach the global (average) error in an iterative fashion. The basic idea of these estimators is that an approximation of the error due to the mesh discretization can be made given the FEA solution and an appropriate better approximation to the continuous stress solution. Adaptive mesh generation can be approached in a variety of ways, the two most common being the h- and p-versions. The h-version improves the accuracy of the solution by refining the mesh, while the p-version uses a fixed mesh but increases the polynomial degree of the shape functions. In the present work the projection type error estimators combined with h-version mesh refinement algorithms which use quadrilateral elements are investigated for two-dimensional linear elastic problems. The

mesh refinement algorithms are based on simple and hierarchical schemes for subdividing quadrilaterals with transitioning, which avoids the need for constraint equations to enforce compatibility at element boundries. Another scheme is based on using constraint equations to enforce compatibility between elements. This h-version will not have as high a convergence rate as a combined h-p-version (or even a p-version), but the h-version is easier to program and the results are easier to interpret,

---

3 Probabilistic Fracture Mechanics

The interest in applying statistics to assess structural reliability has continued to increase. This is evident from the large amount of work in probabilistic fracture mechanics (PFM) and associated topics. Many factors contribute to reliability and these often change both systematically and at random. In the past, structures have been designed using a simple factor of safety approach to calculate a safe lifetime over which the applied loads will be sustained. Each variable in the equations governing the operation of the system was given a reasonable value drawn from past results or even just human intuition, and a predicted life obtained. This was then divided by a factor of safety which reduced it to give a 'safe' maximum operating life. It is conceivable that this is unrealistically conservative but simple.
So that there is a demand, particularly from industry, for a statistical justification behind the calculations, since many parameters may influence the behaviour of a structure and in practice each will be subject to both random and systematic variations.

One approach is to use historical data from past failures and non-failures to evaluate the reliability of current productions.

Thus, an alternative approach has been sought, namely the development and application of engineering models based on an understanding of the failure modes and statistical distributions of the controlling parameters. The latter distributions are not always known, so that errors may be introduced because of poor assumptions.

Ideally, a combination of the two methods is necessary so that past experience and results plus specially designed laboratory tests can be used to obtain statistical distributions which best fit these data, but also, hopefully provide predictions about altered or new systems. The problem is then divided:

1. The basic problem: The two main considerations are the distribution of crack-like defects (or flaws) introduced during the fabrication of a structure and the critical crack length distribution for the material under service conditions, the latter being controlled primarily by the fracture toughness.In general, there is a lack of data for the initial distribution of defects in a structure so the distribution is often assumed to be log-normal or exponential. From a failure point of view, it is importanl to know how this distribution compares with that of the critical crack size, which is controlled by the material properties, and applied loading. The probability of failure is then given by the probability of interaction of the actual crack or flaw a_i, and a critical crack length a_c

In the above, there has been an inherent assumption of independence between a_i and a_c. Marriott and Churchill pose a warning that the presence of defects in regions of low toughness material may potentially increase the failure probability by several orders of magnitude. A preliminary examination of service failures suggests the possibility of a correlation effect may indeed be a real one, not to be ignored.

2. Further considerations: Closely linked with the as-fabricated flaw size distribution is the role played by non-destructive testing in detecting defects which may, or may not, be repaired. Thus, if the initial flaw distribution and the probability of detecting a defect are known, then the distribution of flaws when the structure is put into service can be deduced.

In situations where fatigue cracking occurs, the defect distribution will tend to alter with the number of applied cycles.This problem may be reduced by in-service inspection at fixed intervals of time, and by repairing the defects so found.

3.1 General

The concept of design factors can be pursued in the probabilistic models where the factors themselves are defined in terms of the ratio of characteristic values of load and strength based on statistical models of the variables instead of the mean values. For example, the characteristic value for load may be the 90 percentile value of the load distribution and for strength the 5 percentile value of the strength distribution. (Here,

'90 percentile value' indicates the value below which a load is expected to fall with 90% confidence.) The optimisation of the inherent cost may also be included. Alternatively, the uncertainties of the different loads may be combined statistically, since only one safety factor should be sufficient since there is just one design condition, namely the specified reliability level.

Other approaches include fault tree analysis which is essentially a deterministic approach whereby each event in a sequence is assigned a probability of success/ failure. Fukuda considers this as a link between probabilistic and qualitative methods and explains its use with respect to improving the reliability of welded structures. However, no distribution functions are assumed and so there can be no real consideration of the uncertainties involved. The component probabilities are assumed known, though they may be ill-defined.

In the probabilistic treatment, the random variations are described using distributions of values for the parameters rather than one deterministic value. The distribution may be thought of as a curve combining the possible values and the likelihood (probability) they will occur. The introduction of distributions of values necessarily complicates an analysis, but the end result is likely to be more accurate and hence of more use. In some cases, neat analytical expressions for the reliability are impossible and numerical approximations are required. Approximate interactive algebraic procedures are used to determine an estimate of the failure probability (= 1 - reliability), whereas in the latter, the approximation is at a later stage, after all the exact probabilistic expressions have been obtained for the complete system; this ibe justified by the improvement gained.s, of course, much harder, and the work involved may not be justified by the improvement gained.

3.2 Statistical Basis Of PFM

The basis of PFM is the simple axiom that a given mode of failure event E will occur when the stress σ_w associated with the failure mode exceeds the mode governing strength σ_f. The probability of failure mode E is given by

$$\text{P}(E) = \text{P}(Y < 0) = \text{PD}(y = 0)$$

$$\text{where the strength margin, } Y = \sigma_f - \sigma_w = G(x_i)$$

with $i = 1.....n_x$, depends on input variables that at affect component stress or strength or both. An alternative definition in terms of a strength ratio $Y = \sigma_f/\sigma_w$ is equally valid and leads to P(E) = P((Y)< 1)

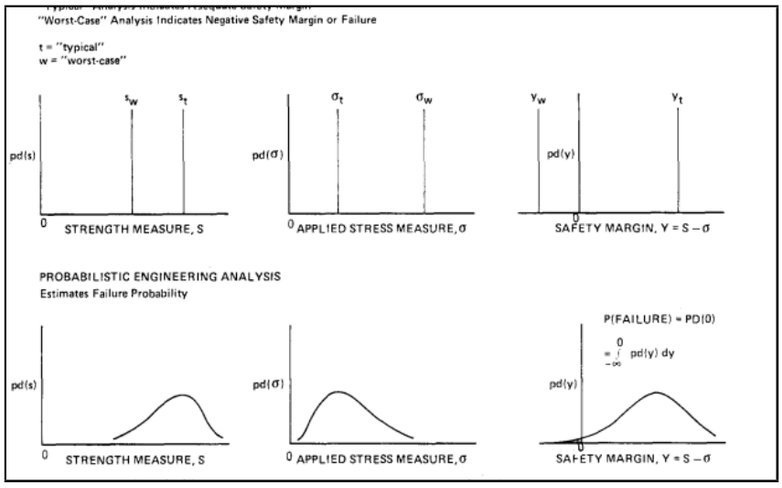

Fig.(a)Contrast between deterministic and probabilistic engineering analysis.

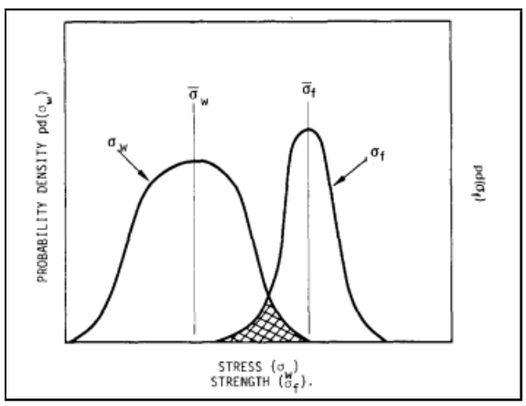

Fig.(b)Statistical variation of strength (σ_f) and applied stress (σ); failure possible over crosshatched region.

Here, G is a concise deterministic summary of all prior engineering experience, models, and assumptions. If the engineering analysis does not lead to an obvious functional form, G may be obtained from standard least- squares fitting of the engineering data or by the repetitive analysis procedure.the x_i are most realistically described as ran dom variables X_i rather than single assigned deterministic values. As shown in fig.(a), statistical interpretation of the X_i results in the interpretation of strength margin as a random variable. The statistical interpretation also allows the analyst to quantify his uncertainty of the engineering model G based on judgement, and his previous record of predictive suc- cess and failure. This error quantification is done by introducing one or more additional X_i to serve as 'error terms'. The cumulative distribution functions of the X_i, represented by

$$\text{PD}(x_i) = \text{P}(X_i \leq x_i)$$

3.3 Flaw Distribution

Perhaps the greatest problem in assessing the reliability of a welded structure is that of data on defects which may be present. Ideally, there should be no defects, but in practice no structure is completely defect free, since no-one is perfect and the result can only be as accurate as the tools available permit, including the experience (or lack of experience) of human operators involved.

In terms of fracture mechanics it is the crack depth that is of importance. Fearnehough and Jones present such data for seamless and seam welded pipe, estimated from preservice pressure test failures. In recent years pipe supplies have been remarkably improved in quality, so alternative information has been obtained by sectioning and measuring all detected defects in a sample of nearly 3000 seamless pipes. The data are similar to those from the failure analysis, but still do not represent the true defect population of an existing pipeline since some defects may have been missed in the inspection and the pressure test will eliminate large unacceptable defects and some smaller insignificant ones.

A way of helping to solve the problem of missing defects is described by Jagger and Manning. The largest defect in each weld is recorded and an extreme value distribution used to model these data. From this, predictions may be made regarding the behaviour of the largest defects, which are expected to be most damaging. Weld defects found in high Temperature steam pipe welds by non- destructive testing (NDT) techniques are analysed in terms of the defect length and depth through the wall thickness to obtain the appropriate distributions.

3.4 Non-Destructive Testing(NDT)

After fabrication, a structure is usually inspected to check for large 'unacceptable' flaws which require repair before service. This inevitably changes the initial defect distribution by filtering some of the larger defects. A general appreciation of NDT is given by Hansen including some of the difficulties encountered. No technique of non-destructive inspection is perfect, so that a probability of detection is associated with each, and this may well vary according to the defects of interest. In terms of fracture mechanics analysis the defect depth is essential, so that an estimate of the accuracy of sizing capabilities must be determined. Packman investigated penetrant systems of aluminium and titanium, which yield greater than 90% ability to detect surface cracks of length greater than 0.939 mm. The probability of detection decreases for small cracks and also varies in accuracy depending on the inspectors' capabilities. Although two may find the same total number of defects (i.e. the same detection probability) one may have a higher percentage of false indications. So, defect detection probability, DDP, is used:

$$\text{DDP} = \frac{\text{Number of teams successfully detecting a particular defect}}{\text{Total number of teams}} \tag{1}$$

3.5 Material Properties

Swindeman claims that he has found that variability in material properties can be traced to differences in chemistry, fabrication and testing procedures. These correlate well with heat-to-heat, product-to-product and laboratory-to-laboratory variability, respectively.

In structures where target failure probabilities are low, it is the extremes of the distributions that are of interest, including the possibility of inconceivable events producing 'outliers' to the distribution.

3.6 Fatigue

Failure by fatigue is a common occurrence in welded joints. Small cracks at weld toes (or the root) may propagate under cyclic loading.It is usually assumed that the stress range versus endurance (S-N) curve is a straight line with two parallel lines. For a particular stress level, S, it is the scatter in fatigue life, N, that is of interest. Therefore, a probability density function for N is required.

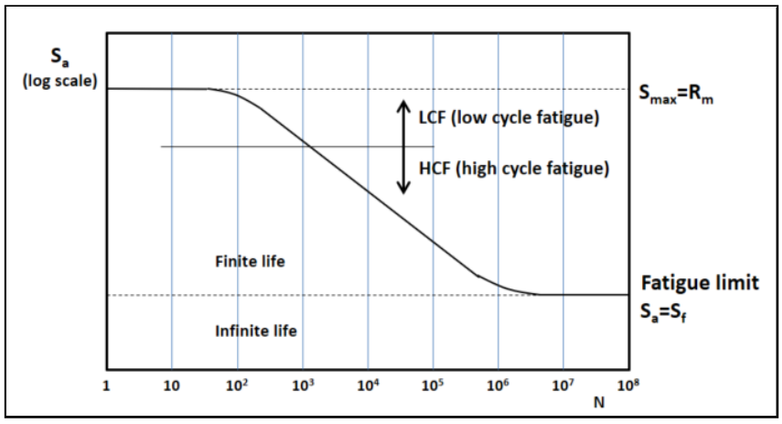

General S-N curve

3.7 Mathematical Techniques

The problem of obtaining sufficient data, upon which statistical predictions for a component may be based, is a real one. Where previous information is available, estimates of sample size may be made using the (previous) sample standard deviation. However, more often, there are no data readily available. Either a guess must be made for the expected variance of the results or sequential testing may be utilised. Smith explains how the method is based on the desired and minimum acceptable reliabilities and the risk involved. After each test, the number of failures and successes is reviewed and a decision made to accept or reject the component or to continue sampling. In general, even when the sample size can be estimated, fewer tests are required using sequential testing. An approximation to the amount of confidence which can be placed in the minimum of a small sample of results is given by Wilks. The equation:

$$\beta^n = 1 - \alpha$$

predicts the percentage, β, of data (from the population) which would be expected to lie above the minimum of n sample results with a confidence of α

---

4 Probabilistic fracture mechanics by using Monte Carlo simulation and the scaled boundary finite element method

In PFM, the sensitivity of the stress intensity stresses are more often than not required to predict the reliability or probability of fracture initiation. Early works in this area include that of which examines probabilistic analysis techniques to estimate the reliability of various response variables, such as the SIF, on the basis of its sensitivity to randomness or uncertainty in the input variables. Commonly used techniques include the Monte Carlo simulation (MCS) method and the first-order reliability method (FORM). For both methods, uncertainties in the applied load, material properties, and crack geometry are modeled as random variables described by specific probability distribution functions. In the MCS methodology, these random variables are generated many times from its distribution function. For each of the Monte Carlo samples, the SIFs, which are sensitive to the randomness of the variables, are computed. The resulting SIFs are compared with the material toughness to evaluate whether failure will occur. Certainly, many deterministic evaluations need to be performed for the MCS method. The method can also be combined with other techniques of fracture modeling such as cohesive elements to perform a reliability analysis. On the other hand, the FORM method requires the mathematical derivative of the SIFs. Evaluation is based on solving an algorithm, such as the Hasofer and Lind algorithm, to linearly approximate the most probable point of failure. Subsequent studies that exercise these procedures. In all of these studies, the sensitivity of the SIF with regards to uncertainties in the applied loads and material properties are shown to be dealt with easily.

the scaled boundary finite-element method is employed to investigate the shape sensitivity of the stress intensity factors of a crack to the size and orientation of the crack. Only a single boundary mesh is required. The variation of the crack size and orientation can be represented by simply changing the position of the crack tip without the need for remeshing the boundary. Therefore, the repetitive deterministic analysis is

made simple, elegant, and highly efficient as compared to most other numerical methods. Thus, it becomes feasible to use the brute force MCS method for the reliability analysis of a cracked structure.

4.1 Scaled Boundary Finite Element Method(SBFEM) For Shape Sensitivity Analysis

4.1.1 Summary of the scaled boundary finite element method for fracture analysis

A 2D homogeneous domain containing a crack tip is illustrated in Figure. The geometry of the domain satisfies the scaling requirement, i.e., the whole boundary of the domain is directly visible from the crack tip. Problems of more complex geometry can be divided into such smaller subdomains. The scaling center O is selected at the crack tip. Without loss of generality, the origin of the Cartesian coordinates $\hat{x}$ and $\hat{y}$ is defined at the scaling center. The boundary is discretized with line elements. The nodal coordinates at the boundary are denoted $\{x\}$ and $\{y\}$, with shape functions $[N(\eta)]$ in the local coordinate η . Thus for any point on the boundary the Cartesian coordinates (x, y), can be interpolated by

$$\begin{aligned} x &= [N(\eta)]\{x\} \\ y &= [N(\eta)]\{y\} \end{aligned} \tag{21}$$

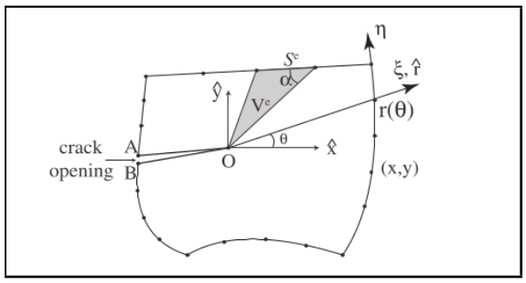

2D cracked plate in scaled boundary coordinate

The domain is generated by scaling the boundary along the radial coordinate ξ pointing from the scaling center O to a point on the boundary. In other words all such boundary line element segments S^e are scaled to the scaling cen ter O to form such and area V^e. By using eq. (21), the coordinates of any point within the domain $(\hat{x}, \hat{y})$ can then expressed as:

$$\begin{aligned} \hat{x} &= \xi x = \xi[N(\eta)]\{x\}; \\ \hat{y} &= \xi y = \xi[N(\eta)]\{y\}; \end{aligned} \tag{22}$$

where the scaling factor ξ takes the value of 0 at the scaling center and 1 on the boundary. ξ and η are called the scaled boundary coordinates. To reiterate, the coordinates of a point in the domain are denoted as $\hat{x}$ and $\hat{y}$ while x and y are researved for the boundary. Note that the two crack faces OA and OB are formed by scaling Points A and B, and thus are not discretized, a distinguishing attribute of the SBFEM for fracture applications. The Jacobian of the coordinate transformation is expressed on the boundary ($\xi = 1$) as

$$[J(\eta)] = \begin{bmatrix} x & y \\ x.\eta & y.\eta \end{bmatrix}$$

To avoid the Jacobian of the scaled boundary coordinate transformation approaching zero, the acute angle formed by a radial line and the boundary should not be too small. As shown in Figure below for a single 2-node element, nodal displacement functions $u(\xi)$ are introduced along the radial lines passing through the scaling center O and a node on the boundary. Along the circumferential direction η , the displacements is obtained by interpolating the nodal displacement functions

$$\{u(\xi, \eta)\} = [N(\eta)]u(\xi)$$

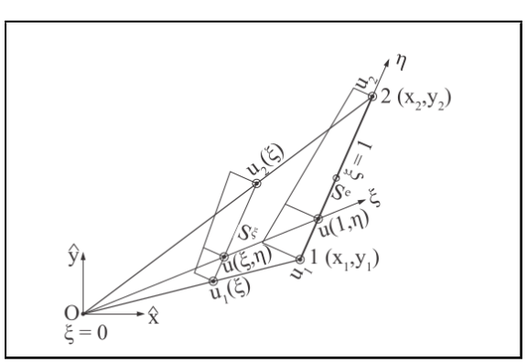

Displacement in scaled boundary coordinates

Applying a weighted residual technique in the η direction leads to the following scaled boundary finite element equation in displacement

$$[E^O]\xi^2\{u(\xi))_{,\xi\xi} + ([E^0] - [E^1] + [E^1]^T)\xi\{u(\xi)\}_{,\xi} - [E^2]\{u(\xi)\} = 0 \tag{23}$$

The global coefficient matrices $[E^0], [E^1]$and $[E^2]$ are obtained by assembling the element coefficient matrices over the complete boundary in the same manner as for the stiffness matrices in the finite element method. The element coefficient matrices are given by

$$\begin{aligned}
[E^0] &= [B^1(\eta)]^T[D][B^1(\eta)]|J(\eta)|d\eta; \\
[E^1] &= [B^2(\eta)]^T[D][B^1(\eta)]|J(\eta)|d\eta; \\
[E^2] &= [B^2(\eta)]^T[D][B^2(\eta)]|J(\eta)|d\eta;
\end{aligned} \tag{24}$$

where $[D]$ is the elasticity matrix. where $[B^1(\eta)]$ and $[B^2(\eta)]$ describe the strain-displacement relationship with

$$[B^1] = \frac{1}{|J|}\begin{bmatrix} y,\eta & 0 \\ 0 & -x,\eta \\ -x,\eta & y,\eta \end{bmatrix}[N(\eta)]$$

$$[B^2] = \frac{1}{|J|}\begin{bmatrix} -y & 0 \\ 0 & x \\ x & -y \end{bmatrix}[N_{,\eta}(\eta)]$$

The displacement functions $u(\xi)$ are expressed as

$$u(\xi) = \sum_{i=1}^{N-1}[\Psi_i^u]\xi^{-[S_i]}\{c_i\} + [\Psi_N^u]\{c_N\} \tag{25}$$

where $[S_i](i = 1, 2, ..., N)$ are diagonal blocks of the real Schur matrix, $[\Psi_i^{(u)}]$ the corresponding displacement modes and c integration constants, which are determined from the displacements on the boundary $u(\xi = 1)$. As in the finite element method, stresses are evaluated element-by-element, yielding the values at a specified local coordinate η within a given element

$$\{\sigma(\xi, \eta)\} = \sum_{i=1}^{N-1}[\Psi_{\sigma i}(\eta)]\xi^{-|S_i|-|I|}\{c_i\} \tag{26}$$

where $[\Psi_{\sigma i}(\eta)]$ represents the stress modes corresponding to the displacement modes $[\Psi_i^{(u)}]$

$$[\Psi_{\sigma i}(\eta)] = [D](-[B^1(\eta)][\Psi_i^{(u)}][S_i] + [B^2(\eta)][\Psi_i^{(u)}]) \tag{27}$$

4.1.2 Evaluation of stress intensity factors

When the real parts of the eigenvalues of a diagonal block $[S_i]$ in Eq. (26) are between -1 and 0, the matrix power function in Eq. (26) leads to a stress singularity. The diagonal block is denoted as $[S^{(s)}]$ (superscript (s) for singular) and $-1 < \lambda[S^{(s)}] < 0$ applies. The corresponding displacement modes and integration constants are denoted as $[\Psi^{(s)}]$ and $\{C^{(s)}\}$Their contribution to stresses vanishes when the limit $\xi \to 0$ is performed and thus are not needed for the definition of stress intensity factors. The singular stress field is expressed as

$$\begin{aligned}
&\{\sigma^{(s)}(\xi, \eta)\} = [\xi_\sigma^{(s)}(\eta)]\xi^{-|S_i|-|I|}\{c^{(s)}\} \\
&\text{where,} \\
&\xi = \hat{r}/r(\theta) \\
&\{\sigma^{(s)}(\hat{r}, \theta)\} = \frac{1}{\sqrt{2\pi L}}(\hat{r}/L)^{-[S^{(s)}(\theta)]}\{K\theta\}
\end{aligned}$$

The SIFs are given by

$$\{K(\theta)\} = \sqrt{2\pi L}[\Psi_{\sigma L}^{(s)}(\theta)]\{c^{(s)}\}$$

4.1.3 Shape sensitivity

The location of the crack tip is perturbed by a finite amount Δa and Δz as shown in Figure below. The scaling center and origin of the coordinates are also moved with the crack tip. This corresponds to the new scaling center $\tilde{O}$ (the effect of perturbation is denoted by accent and domain coordinate translation by

$$\tilde{\hat{x}} = \hat{x} + \Delta a$$
$$\tilde{\hat{y}} = \hat{y} + \Delta z$$

and similarly the nodal coordinate translation by

$$\{\tilde{x}\} = \{x\} + \Delta a$$
$$\{\tilde{y}\} = \{y\} + \Delta z$$

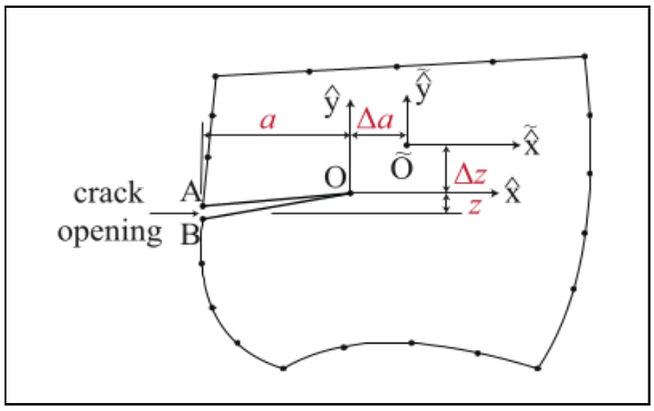

Perturbation in scaled boundary coordinates.

4.2 Fracture Failure Criteria

4.2.1 Mode-I failure

During fracture, the material can be associated with its own characteristic resistance to fracture known as the 'fracture toughness' K_{Ic}such that the crack will grow under Mode-I loading when

$$K_I > K_{Ic}$$

4.2.2 Mixed-Mode Failure

The failure criteria can be simplified, for 2D Mixed-Mode loading, as

$$K_{eff} > K_{Ic}$$

where,

$$K_{eff} = \cos\frac{\theta_c}{2}\left(K_1\cos^2\frac{\theta_c}{2} - \frac{3}{2}K_{II}\sin\theta_c\right)$$

4.3 Monte Carlo Simulation (MCS) method

4.3.1 The deterministic fracture mechanics problem

Assume a high toughness material with crack growth relation, in the range of ΔK values of interest, given by

$$da/dN_{pr} = C\Delta K^n$$

where $C,\ n$ are empirically determined constants, a is the radius of a circular crack in the fracture plane, ΔK is the range of stress intensity factor, and N_{pr} is the number of fatigue cycles. For the case of a buried circular crack remote from the surface and extending through the uniform tensile stress field, we have

$$\Delta K = 2\Delta\sigma(a/\pi)^{1/2}$$

where $\Delta\sigma$ is the range of stress If these equations are combined and integrated, the following expression for fatigue life N_{pr} is obtained:

$$N_{pr} = \frac{a_i^{1-n/2} - a_f^{1-n/2}}{c\Delta\sigma^n(4/\pi)^{n/2}(n/2-1)}$$

where $n \neq 2$, a_i is the maximum initial and a_f is the final half-crack size. The a_f term is negligible for the assumed case of a high toughness material with

$$a_i \ll a_f$$

We may write eq. in terms of the fracture plane defect area $A_i = \pi a_i^2$. The result is

$$N_{pr} = \frac{(A_i/\pi)^{1/2-n/4}}{c\Delta\sigma^n(4/\pi)^{n/2}(n/2-1)}$$

We now consider a buried elliptical crack of fracture plane area $A_i = \pi cb$ where $c \leq b$ are the major and minor semi-axes of the elliptical projection of the flaw on the fracture plane. The results of a more advanced analysis, shows that eq. is reasonably accurate for the elliptical crack, with $b/c \ll 40$, as well as the circular crack of equal area for which eq. is derived. For the purpose of the PFM analysis below, we compact the notation and take the logarithm of eq. to obtain

$$\log N = \log B + p \log C + q \log \Delta\sigma + r \log A_i$$

4.3.2 Distributions of the input random variables $C, \Delta\sigma, A_i$

For simplicity, assume that all previously observed scatter in crack growth rate for given ΔK can be simulated by random variation in C rather than by some complex joint dependent variation of C and n. Previous analyses indicate that this assumption is accurate and produces only minor errors. The relationship

$$da/dN = 6.76 \times 10^{-11} \Delta K^{3.32}$$

is obtained from C r - M o - V steel crack growth data and is used to compute median crack growth rates in in./cyc. For this steel the mean yield stress is $\bar{\sigma} = 85ksi$. The above assumptions can be compacted into the notation

$$\log C = \bar{N}(\mu_c, S_c)$$

that is, log C is a normal random variable with median and mean $\mu_c = \log(6.76X10^{-11})$ and standard deviation S_c . For the example, we further assume a log-normal stress variation of $\log \Delta\sigma = \bar{N}(1.5799, 0.1535)$, which means that Ao has a median value of 38 ksi with 0.1535 standard deviation on log σa due to stress gradients, and spindle-to-spindle design and usage variations. The probabilistic stress distribution shown is formulated from three assumptions. These are (1) log-normality; (2) 95% of the spindle material, by volume, will encounter $\Delta\sigma < 0.80\bar{\sigma}_y$ = 68 ksi; and (3) 95% of the material volume will encounter $\Delta\sigma > .25\bar{\sigma}_y$ = 21 ksi. Finally we assume the flaw size distribution that is used to determine A_i obeys the relation $\log A_i = \bar{N}(-0.9586, 0.750)$.

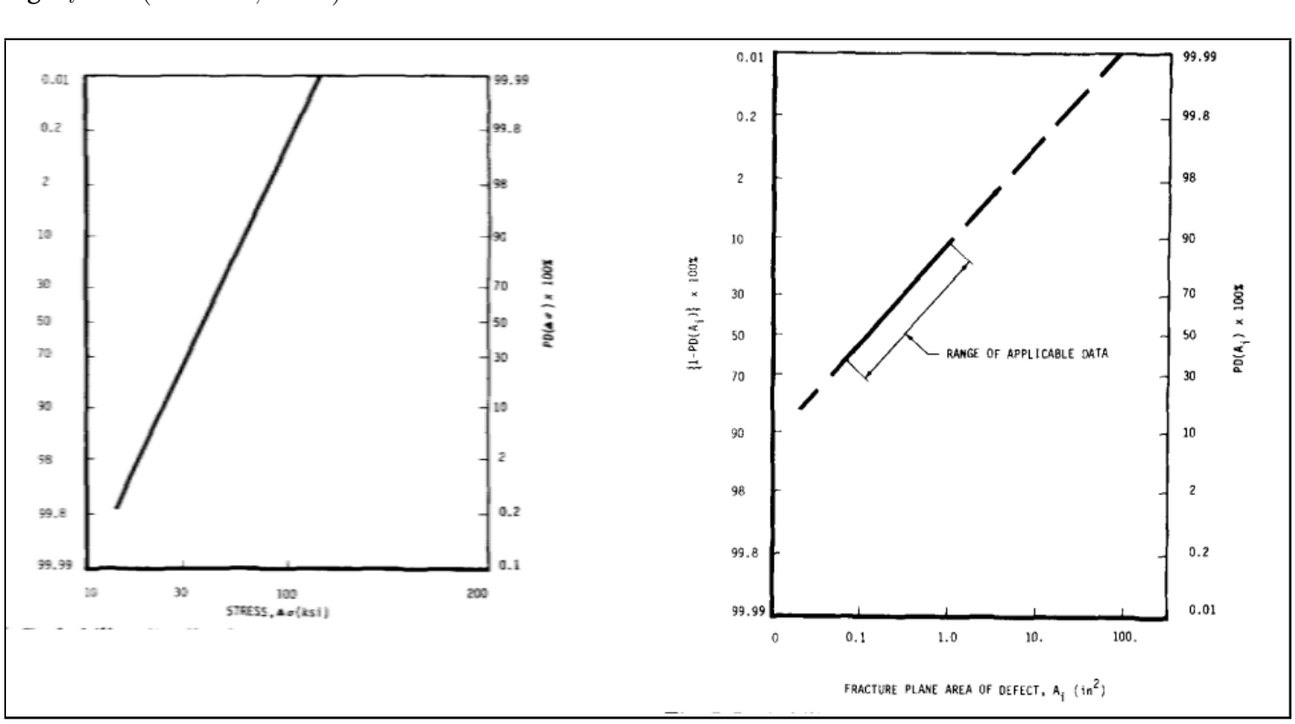

Probability distribution of turbine rotor spindle alternating stress level

4.3.3 The probabilistic analysis

We assume that each rotor spindle must endure the equivalent * of 3000 cycles in service, where each cycle comprises a cold start-up, operation and shut- down. The assumption of constant usage allows a simple definition of Y such as

$$Y = N_{pr} = N_{pr}(C, \Delta\sigma, A_i)$$

and the probability of failure is P(E) = P(Y < 3000 cycles). To obtain an analytical solution for the distribution of fatigue life, we utilize the following theorem

$$X_1 = \bar{N}(\mu_1, S_1), X_2 = \bar{N}(\mu_2, S_2)$$

$$Y = P_1 X_1 + P_2 X_2 + P_3$$

$$Y = \bar{N}(\mu_y, S_y)$$

$$\mu_y = P_1\mu_1 + P_2\mu_2 + P_3$$

$$S_y = (P_1^2 S_1^2 + P_2^2 S_2^2)^(1/2)$$

The numerical results are

$\mu_N \log B + p\mu_c + q\mu_\sigma + r\mu_A = 5.4113$

$S_N = (p^2 S_c^2 + q^2 S_\sigma^2 + r^2 S_A^2) = .5763$

The number of cycles at a given failure probability α is simply

$N_{pr} = 257800(10^{k\alpha})^{.5763}$

and k_α is the standard deviate corresponding to particular α

N_{pr} values (cycles)

PD(N_{pr})	Exact	MC Run 1	MC Run 2	MC Run 3	MMMC*–1	MMMC*–2
10^{-4}	1850				1814	1835
0.001	4270	2045 **	1909 **	5915 **		
0.002	5640	2573 **	5010 **	6394 **		
0.005	8450	5024 **	9270 **	7878 **		
0.01	11 770	8622	12 020	10 650		
0.02	16 750	13 010	17 570	16 850		
0.05	29 060	26 300	27 800	30 180		
0.1	47 040	44 370	49 820	50 218		
0.2	84 300	84 510	89 610	90 843		
0.5	257 800	270 600	271 300	257 900		
0.8	788 000	754 800	830 500	831 800		
0.9	1 410 000	1 270 000	1 544 000	1 401 000		
0.95	2 290 000	1 885 000 **	2 412 000 **	2 197 000 **		
0.98	3 970 000	2 978 000 **	5 274 000 **	4 328 000 **		
0.99	5 650 000	4 676 000 **	6 786 000 **	7 833 000 **		

* In addition to three standard MC runs, 1, 2, and 3 with 1000 simulations each, two additional runs used 1000 simulations each to determine the 10^{-4} fractile of PD(N_{pr}).

4.3.4 Probabilistic addition of crack initiation cycles

The MC program can be utilized to investigate the effect of non-zero initiation life N_i on total fatigue life. For example, the total fatigue life can be written as

$$N = N_i(\Delta\sigma, A_i, D) + N_{pr}(\Delta\sigma, A_i, C)$$

where N_i is proportional to D, a dimensionless random variable with distribution

$$\log D = \bar{N}(0, 0.196)$$

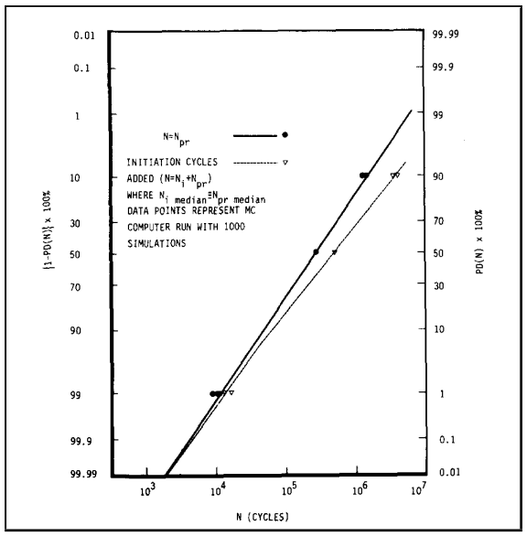

Probability distribution of fatigue lifetime of defected turbine rotor spindle

4.3.5 Direct Monte Carlo Reliability

The Monte Carlo Simulation (MCS) method is widely accepted as a logical tool for modeling structural behavior with significant uncertainties or randomness of input parameters. The execution of the method is very simple and versatile for engineering applications. A N-dimensional random vector **X** with components $\mathbf{X} = (X_1, X_2, ..., X_N)$ characterizing the uncertainties in the input parameters such as the load, crack geometry, and material properties is considered. For instance, if the crack size a, elastic modulus E, the far field applied stress σ^∞ , and the Mode-I fracture toughness K_{Ic} are all random input variables, then $\mathbf{X} = \mathbf{X}(a, E, \sigma^\infty, K_{Ic})$ applies. The structure is deemed to fail if the computed SIF K > K_{Ic} . To be precise, Mode-I failure is dictated by $K_I > K_{Ic}$ while for Mixed-Mode it is $K_{eff} > K_{Ic}$, as mentioned earlier. Clearly, this requirement cannot be satisfied de-terministically as K is dependent on the random vector while K_{Ic} is also random. Note that, rather than depending on customized response surface approximations, the randomness in crack size a is accounted for by the response matrix $[K_s]$ obtained with the SBFEM.
The methodology of the MCS reliability prediction is as follows. The random input variables may or may not be statistically independent of each other. Given their specific statistical parameters, each input variable is randomly generated from some prescribed probability distribution function, based on which the response variable is calculated. This process encompasses 1 MCS cycle and the constituents within the cycle are together taken as 1 sample point. Examples of commonly used distributions for probabilistic analysis include the Gaussian, or normal, distributions defined by

$$f(x) = \frac{1}{\sqrt{2\pi S^2}} e^{-\frac{(x-\mu)^2}{2S^2}}$$

and lognormal distribution is given by

$$f(x) = \frac{1}{x\sqrt{2\pi S^2}} e^{-\frac{(\ln x-\mu)^2}{2S^2}} \tag{28}$$

where $f(x)$ is the probability density function, and S and μ are statistical parameters. The coefficient of variation COV is expressed as

$$COV = S/\mu \tag{29}$$

A large number of such MCS cycles are performed to collect the equal number of sample points. A statistical analysis is carried out for all the sample points to obtain statistical parameters such as the mean μ , standard deviation S, and coefficient of variation COV of the response variable (i.e. SIFs $\{K\}$). Likewise, for each sample an analysis is carried out to evaluate failure, i.e. $K > K_{Ic}$. Letting N_F be the number of simulations when K exceeds K_{Ic} and N to be the total number of simulation cycles, the estimation for the probability that failure has occurred, P_F , can be directly expressed by

$$P_F = \frac{N_F}{N} \tag{30}$$

Inevitably, the MCS method would require a sufficient number of entries in the response matrix [K s] for a reliable probabilistic analysis, particularly when the uncertainty in crack size is very high.

4.3.6 First-Order Second-Moment (FOSM) Reliability

Although it can be determined computationally, the probability of failure P F is also commonly represented by the integral

$$P_F = \int_{g(\mathrm{X})\leq 0} f_{\mathrm{X}}(\mathrm{X}) d\mathrm{X} \tag{31}$$

where X is the vector of random variables, f_{X} (X) is the joint probability density function, and g(X) is the performance function which is given by

$$g(X) = K_{Ic} - K$$

The integral is difficult to evaluate explicitly due to multiple integrals that need to be performed, while the joint probability density function itself is complicated to attain statistically. Often, a first-order approximation technique of the integral is required. A simple example of this is the first-order second-moment (FOSM) method. The controlling characteristic parameter of the FOSM is defined as the Cornell reliability index β

$$\beta = \frac{\mu_{K_{Ic}} - \mu_K}{\sqrt{S^2_{K_{Ic}} - S^2_K}} \tag{32}$$

where μ and S , are the statistical mean values and the standard deviations of the fracture toughness K_{Ic} and stress intensity factor (SIF).Using this index, the probability of failure is approximated by

$$P_F = \phi(-\beta) \tag{33}$$

where $\phi(u)$ is the cumulative probability distribution function and is given by

$$\phi(u) = \frac{1}{\sqrt{2\pi}} \int_{-\infty}^{u} e^{\frac{-t^2}{2}} \tag{34}$$

4.4 Summary Of Monte Carlo Probabilistic Method

The reliability of cracked structures are evaluated by a Monte Carlo probabilistic method. Uncertainties in the crack configuration are modeled using a shape sensitivity approach with the aid of the scaled boundary finite element method (SBFEM). In contrast to the finite element method, efficiency, simplicity, and versatility in achieving this task is recognizable with the SBFEM since no fine internal meshing nor remeshing is necessary for shape sensitivity calculations, noticeably reducing computational effort. Comparative studies show good agreement with results obtained from references. For the same problem, considerably lesser number elements and nodes are required. Indeed, the SBFEM can substantiate for accurate probabilistic fracture analysis. The present technique can also be extended to study the reliability of structures with multi-cracks

---

4.5 Edge-Cracked Plate Under Uniaxial Tension (Mode-I) With Varying Crack Length(Example)

The edge-cracked rectangular plate has dimensions 2L and W. The upper and lower ends of the plate are subjected to tensile stress r 1 . The crack is horizontal and its length a varies. This is an example of a Mode-I problem.

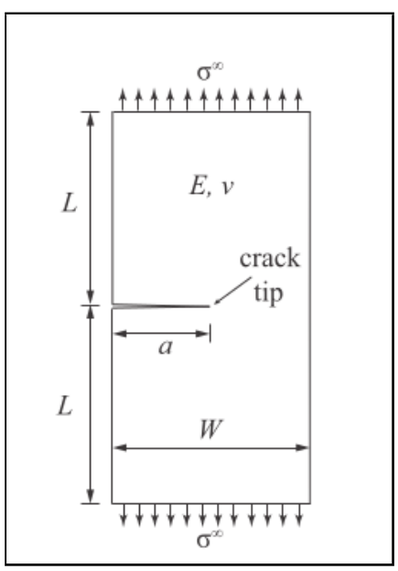

Horizontal edge-cracked plate under uniaxial tension

4.5.1 Shape Sensitivity Analysis

Coinciding with $g(X) = K_{Ic} - K$, the dimensions of the plate is chosen as $L/W = 1$ with far-field applied tensile stress σ^{∞} = 1 unit. The elastic material properties are taken as Young's modulus$E = 20.7x10^6$units and Poisson's ratioν = 0.3. The normalized crack length a/W is varied from 0.1-0.8. For relatively small crack sizes $a/W \leq 0.2$ the rectangular plate is divided into 3 sub-domains (Fig. a) with 14 elements (210 nodes), while for larger crack sizes $0.2 < a/W \leq 0.8$ only 1 sub-domain is used (Fig. b) with 12 elements (190 nodes).

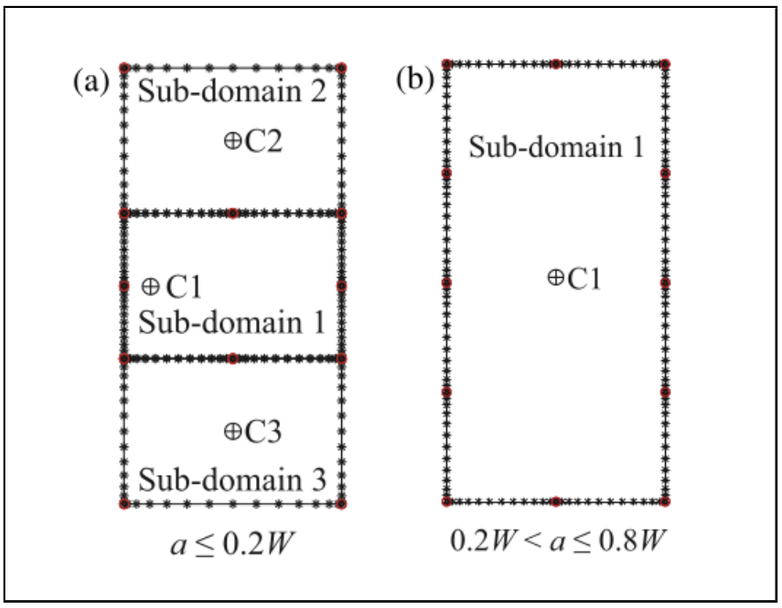

Mesh of horizontal edge-cracked plate: (a) 3 sub-domain mesh; (b) 1 sub-domain mesh.

The computed normalized Mode-I stress intensity factor (SIF) $K_1/\sigma\sqrt{\pi a}$ is plotted as a variation of the normalized crack length a/W . Note that this is reflective of the Mode-I response matrix $[K_s]$. Acceptable convergence is achieved using 9-node, 11-node, and 15-node elements . The corresponding derivative $\partial K_I/\partial a$ is calculated and plotted. Analytical solutions are also provided for an infinite domain (i.e. $L/W = \infty$).

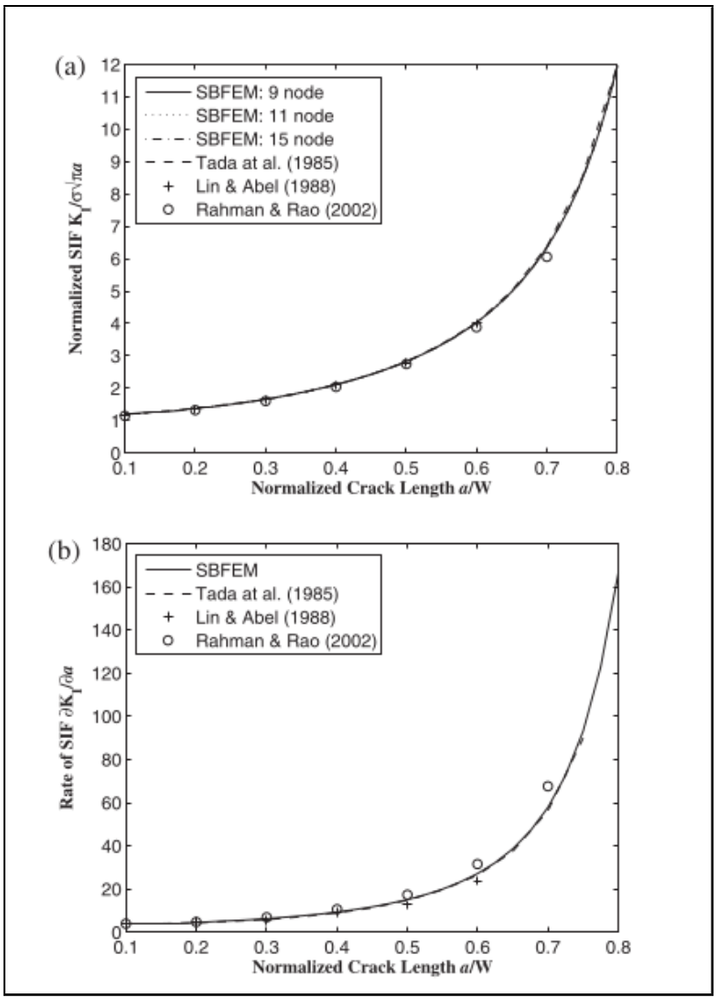

Horizontal edge-cracked plate under uniaxial tension: (a) normalized Mode-I (b) rate of Mode-I

Probabilistic analysis A probabilistic analysis is carried out for the same plate. Adopting the dimensions of the plate are taken to be W = 0.508 m and 2L = 5.08 m (i.e.$L/W = 5$) with randomness (uncertainty) in the applied farfield tensile stress of r 1 , crack length a, Young's modulus E and Poisson's ratio ν , and fracture toughness J_{Ic} . The Mode-I response matrix $[K_s]$ is calculated using the scaled boundary finite element method (SBFEM). For the sake of comparison with the aforementioned reference, the value of the J-integral, yet another fracture parameter commonly used in probabilistic analysis, is determined by the Griffith-Irwin relation given as $J = K^2/E$ for the plane stress condition. The load, crack size, and material properties are treated as statistically independent random variables. The Monte Carlo simulation (MCS) method is used to determine the probability of failure P F . The mean far-field tensile stress is indicated as $E[\sigma^{\infty}]$ where E[.] is the expectation (mean) operator. Figure plots the probability of failure P F VS . the mean far-field tensile stress $E[\sigma^{\infty}]$ for both the deterministic ($COV^{a/W}$ = 0%) and random ($COV^{a/W}$ = 5%, 10%, and 15%) crack sizes. As expected, the results indicate that the failure probability increases with the $COV^{a/W}$ (uncertainty).The failure probability can be much larger than the probabilities calculated for a deterministic crack size, particularly when the uncertainty of a/W is large.

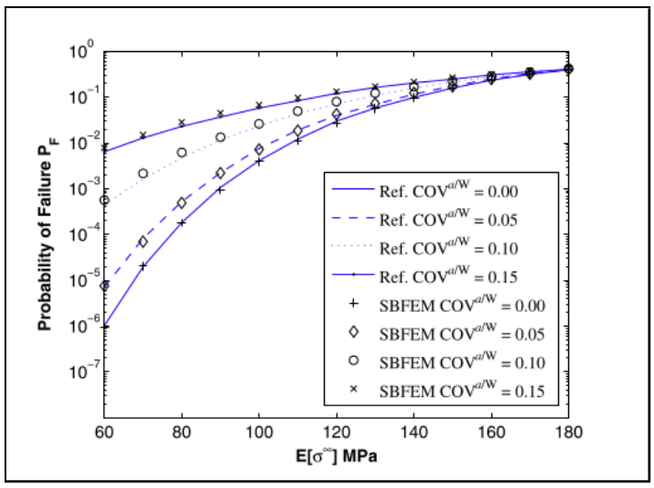

Failure probability of horizontal edge-cracked plate under uniaxial tension for varying uncertainty

---

5 Conclusion

⇒ Fracture initiation and stable crack growth are local fracture phenomena. Therefore, in order to apply the energy principle, the variation of the local crack tip stresses and strains and the associated detailed fracture process have to be taken into consideration

⇒ Fracture toughness is the measure of the fracture ductility of a material. The fracture ductility of a material is a function of the superimposed hydrostatic tensile stress. The tearing modulus is the measure of the increase in fracture ductility as the hydrostatic tension is reduced when the fr icture surface changes from mode I to a combination of modes I, II, and III during stable crack growth.

⇒ In order to extend fracture mechanics beyond the realms of K and J, the fracture mechanism has to be found, the crack tip stress and/or strain directly responsible for the fracture process has to be established, and the local stresses and strains have to be related to far field parameters.

⇒ The stress smoothing error estimators highlighted in this work seem to offer many advantages. They appear to be robust and efficient. Further work is needed in comparing these and other estimators so that they can be incorporated into a commercial adaptive FE program. There are many other areas of the adaptive FEM that need to be investigated, such as error estimators, solution algorithms, extension to three dimensions, non-linear and dynamic analyses and the incorporation of these in an optimized user-friendly environment using ideas of knowledge-based systems and expert systems for fracture-proof design

⇒ A probabilistic fracture mechanics (PFM) analysis is often necessary in order to achieve accurate estimates of reliability of structural components and to study the effects on reliability of systematic and stochastic variation in controlling parameters.

⇒To enhance future PFM applications, data collection efforts should seek to quantify the variational characteristics and the uncertainties of the studied parameters. In this manner, a data base of input parameter probability distributions can be formed to facilitate future PFM and other engineering probability and risk analyses.

⇒ The reliability of cracked structures are evaluated by a Monte Carlo probabilistic method. Uncertainties in the crack configuration are modeled using a shape sensitivity approach with the aid of the scaled boundary finite element method (SBFEM). In contrast to the finite element method, efficiency, simplicity, and versatility in achieving this task is recognizable with the SBFEM since no fine internal meshing nor remeshing is necessary for shape sensitivity calculations, noticeably reducing computational effort. Comparative studies show good agreement with results obtained from references. For the same problem, considerably lesser number elements and nodes are required. Indeed, the SBFEM can substantiate for accurate probabilistic fracture analysis. The present technique can also be extended to study the reliability of structures with multi-cracks.

Biblography

[1] H. W Liu, "*On the fundamental basis of fracture mechanics*", Engineering Fracture Mechanics Volume 17, Issue 5, 1983, Pages 425-438, https://doi.org/10.1016/0013-7944(83)90039-5

[2] H. Liebowitz, J. S. Sandhu, J.D. Lee, F.C.M.Menandro, "*Computational fracture mechanics: Research and application*", Engineering Fracture Mechanics Volume 50, Issues 5–6, March–April 1995, Pages 653-670, https://doi.org/10.1016/0013-7944(94)E0051-H

[3] P. M. BesunerA, S. Tetelman, "*Probabilistic fracture mechanics*", Nuclear Engineering and Design Volume 43, Issue 1, August 1977, Pages 99-114, https://doi.org/10.1016/0029-5493(77)90134-0

[4] Morsaleen Shehzad Chowdhury, Chongmin Song, Wei Gao, "*Probabilistic fracture mechanics by using Monte Carlo simulation and the scaled boundary finite element method*", Engineering Fracture Mechanics Volume 78, Issue 12, August 2011, Pages 2369-2389, https://doi.org/10.1016/j.engfracmech.2011.05.008

[5] G. O. Johnston, "*A review of probabilistic fracture mechanics literature*", Reliability Engineering Volume 3, Issue 6, November 1982, Pages 423-448, https://doi.org/10.1016/0143-8174(82)90035-X